

Evaluation of the surface treatment effect on the corrosion performance of paint coated carbon steel

D.M. Santágata, P.R. Seré, C.I. Elsner, A.R. Di Sarli*

Centro de Investigación y Desarrollo en Tecnología de Pinturas (CIC-CONICET), Av. 52, 121 y 122, CP 1900 La Plata, Argentina

Received 5 December 1996; accepted 9 October 1997

Abstract

Electrochemical impedance spectroscopy studies were carried out for plasticized chlorinated rubber coated carbon steel sheets under free corrosion conditions when exposed to artificial seawater. Four different sample types were used (sandblasted, pickled, pickled + phosphatized and sandblasted + wash primer). Electrochemical impedance spectroscopy (EIS) data was interpreted considering the values of the distinct equivalent electrical circuit models, whose components allowed a quantitative evaluation of the long term corrosion behavior for the different pretreated coated steel specimens. Furthermore, from impedance data, the water content of the paint on the steel substrate was calculated by the Brasher expression and the progress of the coating delamination process was calculated by an empirical expression relating to the measured/specific double layer capacitance ratio. On the basis of both the electrochemical and the visually monitored test results it was concluded that the best corrosion performance was provided by pickled + phosphated painted steel surfaces followed by the pickled surfaces. This result was attributed to the fact that such surface treatments might improve the barrier protection and the steel/paint adhesion properties or reduce the osmotic pressure effect, respectively. © 1998 Elsevier Science S.A.

Keywords: Surface treatments; Painted carbon steel; Impedance measurements; Water uptake; Delaminated area; Equivalent circuits

1. Introduction

Surface preparation and/or pretreatment is always important in obtaining satisfactory coatings performance. It is particularly critical for immersion or high humidity conditions, which are unforgiving of mistakes in surface preparation and coating application. Coatings must be able to form a barrier in order to break the metal–electrolyte connection for delaying or stopping the metallic substrate corrosion reaction. With these characteristics and others mentioned later, based on the film strong properties, it is little wonder that the chlorinated rubber, which is a compound formed by reacting natural rubber with chlorine, has found so much use as a maintenance coating vehicle over the years. Thus, coatings made from chlorinated rubber that have been blended with highly chlorinated additives provide toughness, water impermeability and chemically resistant properties. As a consequence, heavy-duty coating systems based on this

polymer are being used extensively in the protection and decoration of chemical plants, refineries, pipelines, bridges, power generation and many other (power transmission, harbor, marine, etc.) facilities. As no paint is indestructible, all the organic coatings will undergo normal deterioration with time, however, its rate can be slowed significantly by choosing a top quality coating and/or using the appropriate surface preparation and application technique.

Water and oxygen can permeate, at least to some extent, through any organic film although it has no intrinsic structural defects such as cracks and/or pores through the film. Water and oxygen travel through the film by jumping from one free volume hole to other.

As part of a program aimed at defining a lifetime prediction model for steel sheets coated with an organic film, an investigation related to the role played by the surface pretreatment given to the substrate on the global deterioration of such systems has been started. Therefore, the purpose of the present paper is to study the differences in the corrosion protection and coating disbondment provided by a chlorinated rubber paint applied to previously treated (sandblasted

* Corresponding author.

(S), pickled (P), pickled + phosphated (PPh) or sandblasted + wash primer (SWP)) carbon steel sheets in artificial seawater. This steel was chosen because it is a commonly used structural material which requires protection against corrosive environments. Electrochemical impedance spectroscopy (EIS) measurements were carried out to understand the effect, if any, of the surface preparation method on the corrosion protective properties afforded by a chlorinated rubber paint (30 and 80 μm in thickness), plasticized with chlorinated paraffin and pigmented with titanium dioxide. Periodical visual inspections were also carried out.

2. Experimental procedure

Each sample substrate consisted of a ($10 \times 10 \times 0.3$ cm) carbon steel test panel, whose chemical composition (%) was: C (0.16), Mn (0.54), Si (0.05), S (0.01), P (0.01), with Fe being the difference. The surface treatment procedures for steel were: (1) sandblasted to ASa 2 1/2–3 (Swedish Standard SIS 05 59 00/67) and its roughness, measured with a Hommel Tester Model T 1000, was $2.04 \pm 0.24 \mu\text{m}$; (2) pickled in HCl inhibited with tetrabutyl ammonium iodide + phosphated, using a bath based on a ZnO and H_3PO_4 – HNO_3 mixture at 95°C for 30 min; (3) pickled in inhibited HCl and (4) sandblasted + wash primer based on a vinyl resin pigmented with zinc tetroxy chromate. Then, the steel sheets were cleaned with toluene to ensure surface uniformity and coated with a commercially available chlorinated rubber prepared by addition of 70% chlorinated rubber 20cP, plasticized by addition of 30% chlorinated paraffin and pigmented with TiO_2 . Specimens were coated using a Bird applicator which gave uniform coating thicknesses. The average dry film thicknesses (30 or 80 μm for thin and thick films, respectively) were measured using an Elcometer Model 300 electromagnetic gauge, Table 1. Two acrylic tubes used as electrolyte vessels were fixed to the intact coated steel sheet with an epoxy adhesive. The geometrical area for each cell exposed to the electrolyte was 15.9 cm^2 . A Pt–Rh mesh and a saturated calomel electrode (SCE) were used as counter- and reference electrodes, respectively. The cell was filled with artificial seawater pre-

pared according to the ASTM Standard D-1141/94 to a depth of 9 cm.

All impedance spectra in the frequency range 10^{-3} – 3×10^5 Hz were performed in the potentiostatic mode at the corrosion potential as a function of the exposure time to the electrolyte solution, using a 1255 Solartron Frequency Response Analyzer and a 1286 Solartron Electrochemical Interface. The amplitude of the applied AC voltage was 10 mV peak to peak. Data processing was accomplished with a PC and a set of programs developed at CIDEPINT [1] and by Boukamp [2].

3. Experimental results

3.1. Water uptake

Water absorption by an organic coating leads to changes in the film's mechanical and electrical properties, i.e. a reduction in the adhesion and/or cohesion forces as well as the electrical resistance. Many authors [3–5] have studied the water uptake process using impedance measurements for evaluating the organic coating capacitance trend when immersed in an aqueous solution. The significance of such evaluation arises from the fact that this phenomenon is related to the corrosion protection properties, which can be determined from EIS data.

As the water permeates, the dielectric constant of the polymer changes and, therefore, the coating dielectric capacitance (C_f) does too. In this way, the coating capacitance evolution allows the water uptake evaluation using, for instance, an expression derived by Hartshorn, Megson and Rushton [6] and employed by Brasher [7] to obtain the following empirical equation:

$$X = \frac{\log(C_f(t)/C_f(0))}{\log 80} \quad (1)$$

where X is the volume fraction of water absorbed, $C_f(0)$ and $C_f(t)$ are the organic coating dielectric capacitances measured just after immersion ($t = 0$) and at any time t , respectively and $\log 80$ is the logarithm of the water dielectric constant at 25°C .

Table 1

Coatings thickness

Sample	Thickness (μm)	Sample	Thickness (μm)	Sample	Thickness (μm)	Sample	Thickness (μm)
P ₁	30	S ₁	30	PPh ₁	30	SWP ₁	30
P ₃	30	S ₃	30	PPh ₃	30	SWP ₂	30
P ₅	30	S ₅	30	PPh ₆	30	SWP ₃	30
P ₇	30	S ₇	30	PPh ₈	30	SWP ₅	30
P ₉	30			PPh ₁₀	30	SWP ₇	30
P ₂	80	S ₂	80	PPh ₂	80	SWP ₉	30
P ₄	80	S ₄	80	PPh ₄	80	SWP ₄	80
P ₆	80	S ₆	80	PPh ₅	80	SWP ₆	80
P ₈	80			PPh ₇	80	SWP ₈	80
P ₁₀	80			PPh ₉	80	SWP ₁₀	80

Figs. 1f, 2f, 3f and 4f show the water absorption of chlorinated rubber coatings deposited on steel sheets subjected to different surface preparation procedures and exposed to artificial seawater. From these data it was possible to obtain values of water uptake saturation ranging between 0.5 and 3%.

3.2. Corrosion potential

Figs. 1a, 2a, 3a and 4a illustrate the corrosion potential (E_{corr}) changes measured in the coated steel sheets for 70 days of exposure. It is evident that, in general, the potential of the pickled (P), pickled + phosphated (PPh) and sandblasted + wash primer (SWP) samples, coated with the

thicker paint films remain almost constant and close to 0 ± 0.1 V/SCE. On the other hand, samples coated with a thinner film as well as all the sandblasted (S) samples exhibit values which either remain stable or vary to the normal E_{corr} for unprotected steel under these experimental conditions of -0.6 ± 0.1 V/SCE. This behavior reflects certain areas of exposed metal. In essence, the more negative the measured potential becomes, the more susceptible to corrosion is the underlying steel surface.

3.3. Equivalent circuit models

Impedance spectra provide important information related to both the organic coating deterioration evolution and the

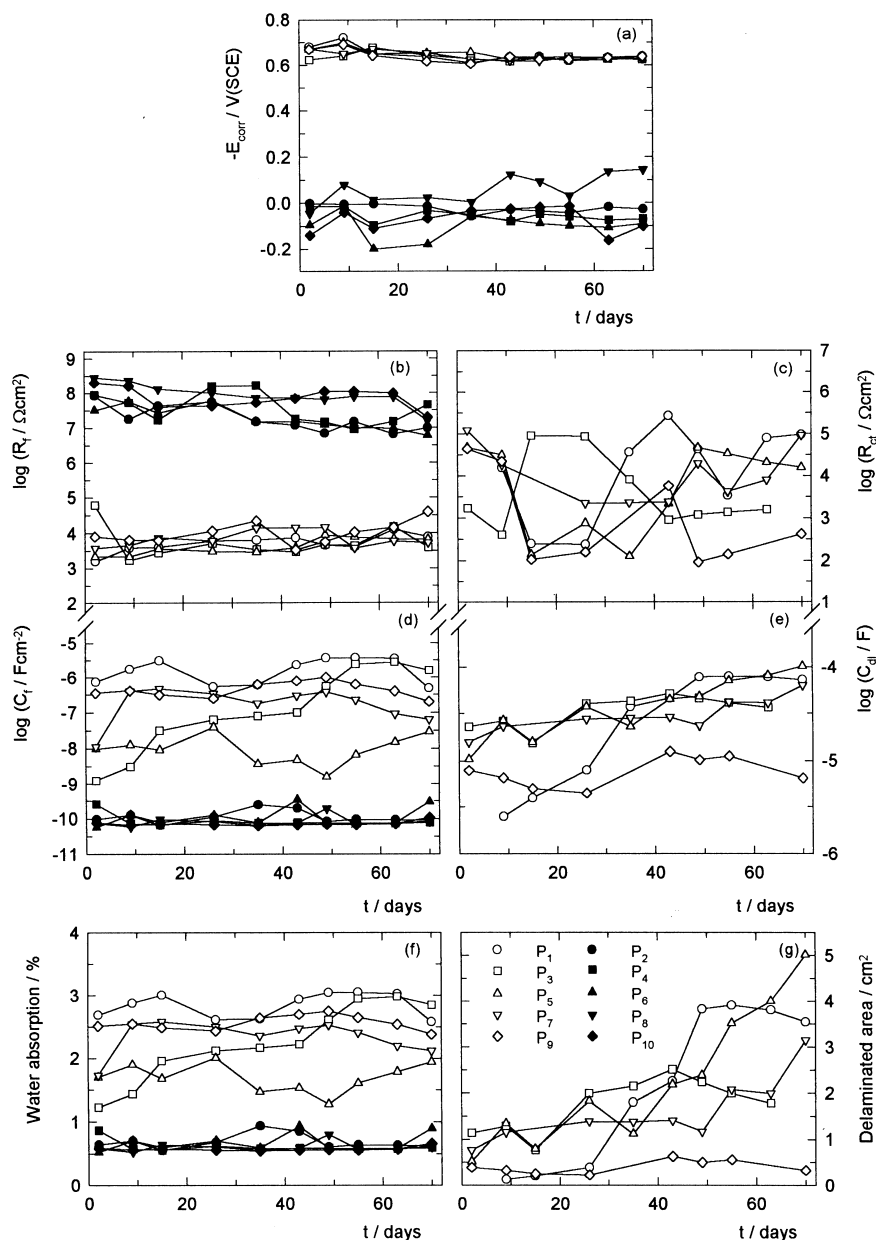


Fig. 1. Time dependence of the different parameters characterizing the sandblasted painted steel/artificial seawater system performance. White and black symbols indicate experimental results for 30 and 80 μm thick chlorinated rubber paint, respectively.

kinetics of the corrosion process occurring on the underlying steel substrate. The dynamic character of both the paint film conductivity and the corrosion products (basically rust) formation as well as the shifts in the disbonded area account for changes in the coated steel/electrolyte systems impedance spectra throughout the immersion time. In order to give a physical explanation of such changes and to obtain a more accurate and less consuming time curve fitting procedure, the equivalent circuit models shown in Table 2 have to be used. They represent the parallel and/or series connection of a number of resistors and capacitors, simulating a heterogeneous arrangement of electrolytically conducting paths. At the beginning of the exposure there is no solution at the

steel/paint interface, therefore, neither electrochemical double layer nor faradaic reaction occur. The information coming from impedance data is associated with the organic coating properties. Thus, R_s represents the electrolyte resistance between the reference (SCE) and working (coated steel) electrodes. R_f is the resistance to the ionic flux and describes paths of lower resistance to the electrolyte solution penetration short-circuiting the organic coating, its value is usually used as a criterion of coating integrity. C_f is the dielectric capacitance and its value is associated with the membrane water uptake [8], (circuit A). At longer exposure times, permeated corrodent species such as water, oxygen and ions increase the coating conductivity in such a way

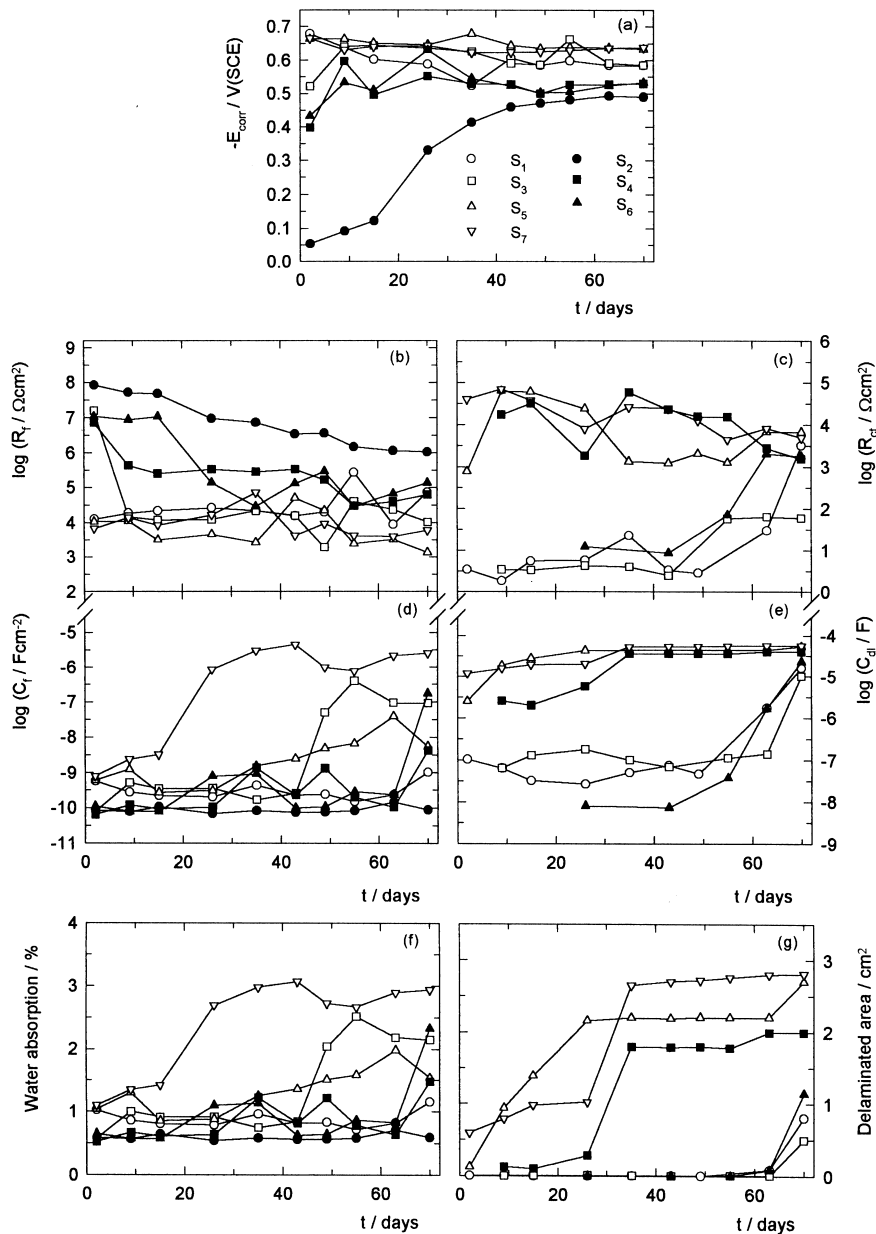


Fig. 2. Time dependence of the different parameters characterizing the pickled painted steel/artificial seawater system performance. White and black symbols indicate experimental results for 30 and 80 μm thick chlorinated rubber paint, respectively.

that not only the R_f and C , but also a diffusional component Z_d – which was related to the relaxation of a mass transport process linked to the oxygen reduction reaction [9] – become measurable. The latter masks completely the initial corrosion attack presumably taking place at a highly localized steel area, (circuit B). Then, once the permeating species reach more significant electrochemically active areas of the substrate, the corrosion process becomes measurable so that the electrochemical double layer C_{dl} and the charge transfer resistance R_{ct} – proper of the faradaic process – can be estimated, (circuit C). In turn, this circuit can be connected with the diffusional component Z_d in series with R_{ct} , (circuit D).

Sometimes, when the time constants (RC or RQ couples) corresponding to the anodic and cathodic reactions do not overlap, these components together with the diffusional one have to be used in order to get the best data fit, (circuit E).

Distortions observed in the resistive–capacitive contributions indicate a deviation from the theoretical models in terms of a time constant distribution. This effect is caused by paint film structural heterogeneities, lateral penetration of the electrolyte at the steel/chlorinated rubber paint interface (usually starting at the base of the coating defects), underlying steel surface heterogeneities (topology, chemical composition, surface energy) and/or diffusional processes that can take place along the test [10,11]. These

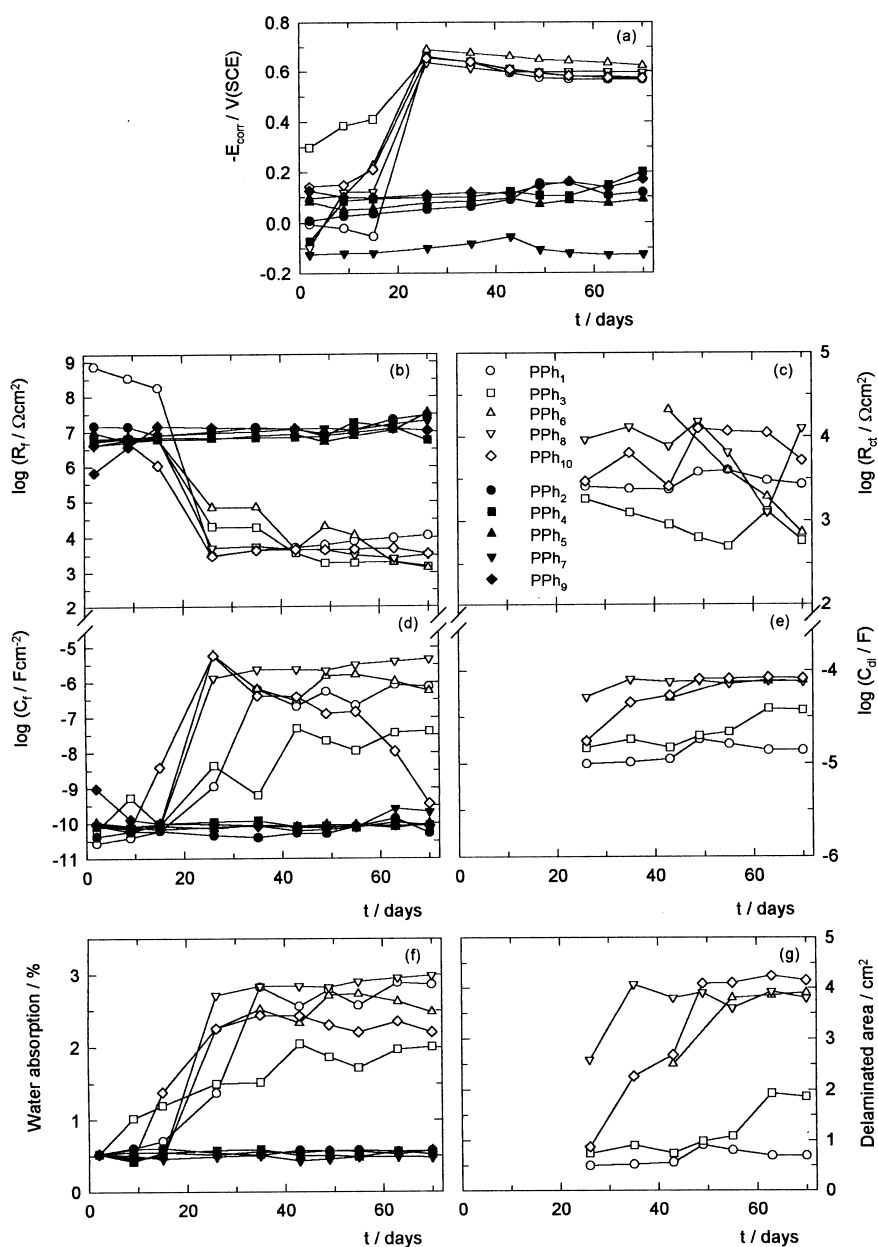


Fig. 3. Time dependence of the different parameters characterizing the pickled + phosphated painted steel/artificial seawater system performance. White and black symbols indicate experimental results for 30 and 80 μm thick chlorinated rubber paint, respectively.

factors are taken into consideration during the fitting of the transfer function associated with the most probable equivalent circuit using the constant phase element Q_i . However, difficulties in providing an accurate physical description of the occurring processes are sometimes found. In such cases, the standard deviation value of the fitting procedure is used as the final criterion to define the most probable circuit.

3.4. Impedance results

The time dependent values of the equivalent circuit elements corresponding to the steel pretreated/chlorinated rubber paint/artificial seawater systems modeled by some of the

impedance networks shown in Table 2, are summarized in Figs. 1b–e, 2b–e, 3b–e and 4b–e and Table 3.

The loss of the barrier protective properties, particularly faster in the thinner polymer films, causes either decreasing or very low R_f values in the case of P, PPh and SWP as well as in almost all the S samples, (Figs. 1b, 2b, 3b and 4b). At initial times, most of the R_f values for the thicker coatings are at or above $10^7 \Omega \text{ cm}^2$, regardless of the pretreatment applied. While the corresponding values for the thinner coatings are highly variable ranging from 10^3 to $10^8 \Omega \text{ cm}^2$. As the test proceeds, the ionic resistance decreases to a magnitude depending on the steel surface pretreatment, except for the thicker coatings applied on PPh samples

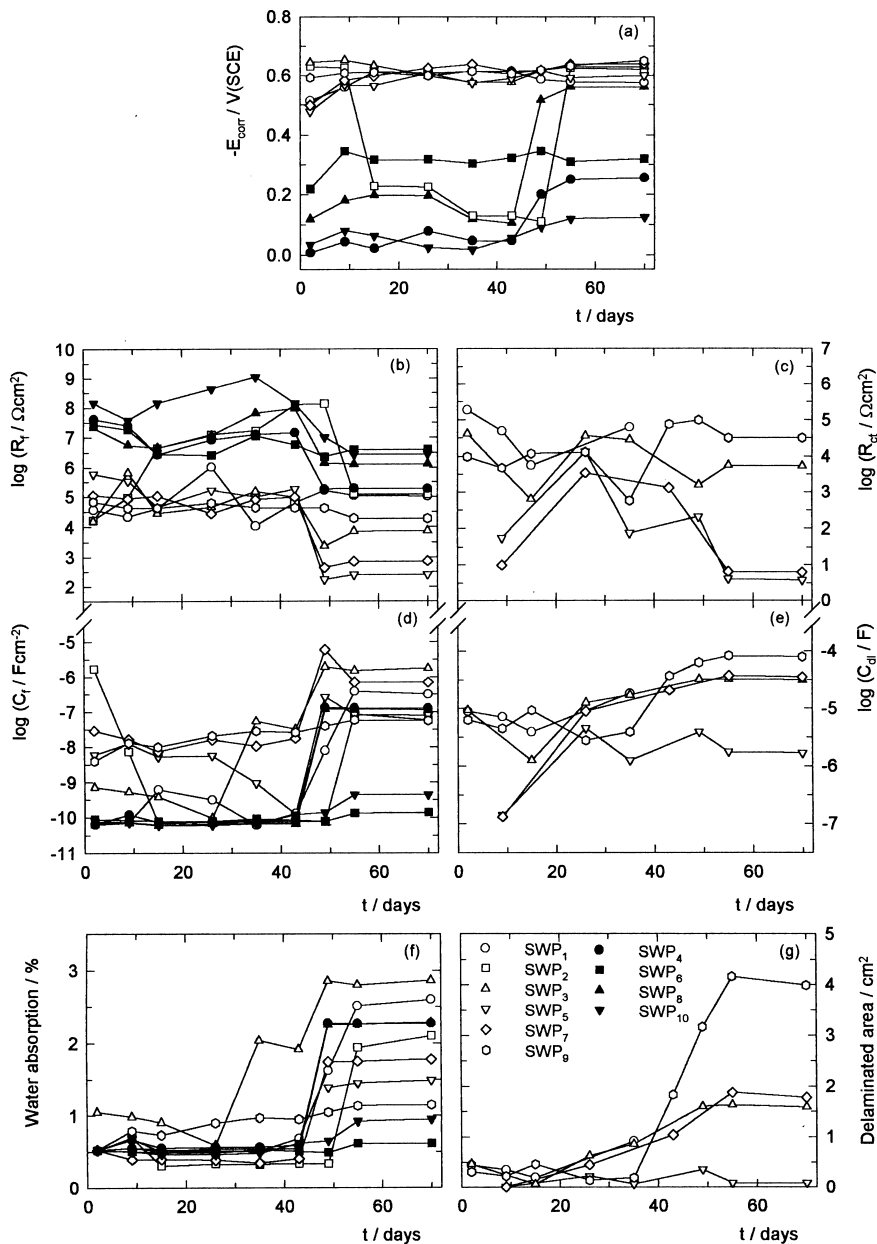
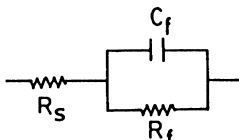
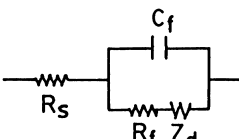
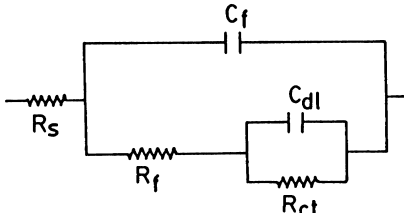
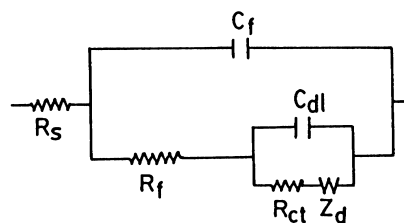
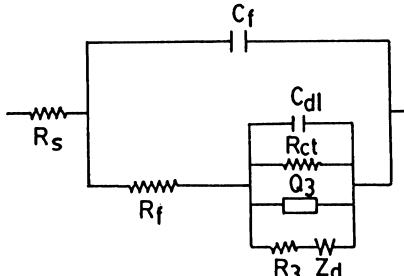


Fig. 4. Time dependence of the different parameters characterizing the sandblasted + wash primer painted steel/artificial seawater system performance. White and black symbols indicate experimental results for 30 and 80 μm thick chlorinated rubber paint, respectively.

which do not change. Such a result is indicative of an increasing coating layer ionic conductivity, and presumably a lower protective capacity caused by the electrolyte penetration. For instance, Fig. 3 summarizes the coating resistance R_f and capacitance C_f , the coated steel E_{corr} , the charge transfer resistance R_{ct} and the electrochemical double layer capacitance C_{dl} , as well as the membrane water absorption percentage and the delaminated area dependence on time for the pickled + phosphated painted steel. Whether the metal substrate is coated with a thick or a thin paint film, R_f starts

at a value of about $10^7 \Omega \text{ cm}^2$, but in the latter case it drops to $\cong 10^4 \Omega \text{ cm}^2$ after 25 days of exposure. Fig. 3 also shows that these changes correlate well with the E_{con} displacement towards more active values as well as with the increase in the coating capacitance and the amount of water absorbed. Furthermore, it is interesting to denote that from the moment the mentioned changes occurred, the R_{ct} and C_{dl} values become calculable, indicating not only the presence of a significant corrosion process but also the end of an effective coating barrier protection at the point from

Table 2
Impedance networks used to fit experimental data

Circuit	Samples			
	S	P	PPh	SWP
A	27	45	62	50
				
B	3	17	1	10
				
C	22	5	19	15
				
D	7	18	3	10
				
E	16	7	5	6
				

Numbers in columns indicate the times that each network was used throughout the test.

Table 3

Evolution of the electrochemical parameters assumed to be associated with the cathodic processes

<i>t</i> (Days)	2	9	15	26	35	43	49	55	63	70
<i>Sample S1</i>										
$R_3 \times 10^{-5}$ ($\Omega \text{ cm}^2$)						3.29	13.70		0.26	0.36
$Q_3 \times 10^6$ (F/cm ²)						0.79	2.68		3.22	1.30
$Z_d \times 10^6$ (F)	1.90	3.19	5.14	13.60					156	
<i>Sample S3</i>										
$R_3 \times 10^{-5}$ ($\Omega \text{ cm}^2$)		0.74	6.15	3.13		1.55				0.08
$Q_3 \times 10^7$ (F/cm ²)		3.46	3.82	6.29		13.40				17.20
$Z_d \times 10^5$ (F)		2.07	5.07							20.70
<i>Sample S4</i>										
$R_3 \times 10^{-4}$ ($\Omega \text{ cm}^2$)				31.00					0.10	7.55
$Q_3 \times 10^6$ (F/cm ²)				0.34					2.05	4.10
$Z_d \times 10^5$ (F)							7.82			
<i>Sample S5</i>										
$R_3 \times 10^{-5}$ ($\Omega \text{ cm}^2$)	12.50					0.72	0.40			
$Q_3 \times 10^7$ (F/cm ²)	5.22					24.30	3.52			
$Z_d \times 10^5$ (F)					7.31			8.50		
<i>Sample S6</i>										
$R_3 \times 10^{-4}$ ($\Omega \text{ cm}^2$)						23.80				7.68
$Q_3 \times 10^7$ (F/cm ²)						0.16				120
$Z_d \times 10^6$ (F)				5.69						
<i>Sample S7</i>										
$R_3 \times 10^{-4}$ ($\Omega \text{ cm}^2$)				20.30		8.22		7.29		
$Q_3 \times 10^6$ (F/cm ²)				1.35		3.17		2.59		
<i>Sample P1</i>										
$R_3 \times 10^{-5}$ ($\Omega \text{ cm}^2$)			7.07					7.41		
$Q_3 \times 10^7$ (F/cm ²)			15.60					7.55		
$Z_d \times 10^6$ (F)	34.50						6.02			
<i>Sample P3</i>										
$R_3 \times 10^{-5}$ ($\Omega \text{ cm}^2$)	27.00	3.13	0.03	0.36	7.25	4.08	9.85		1.20	
$Q_3 \times 10^7$ (F/cm ²)	0.20	2.51	5.59	5.78	6.79	16.8	14.9		9.18	
$Z_d \times 10^5$ (F)					8.69			2.82		
<i>Sample P5</i>										
$R_3 \times 10^{-6}$ ($\Omega \text{ cm}^2$)			0.70	1.16	2.92					
$Q_3 \times 10^6$ (F/cm ²)			3.94	2.66	1.17					
<i>Sample P7</i>										
$R_3 \times 10^{-5}$ ($\Omega \text{ cm}^2$)								3.70	1.53	
$Q_3 \times 10^6$ (F/cm ²)								2.83	4.66	
$Z_d \times 10^5$ (F)			2.12	4.30	8.05					
<i>Sample P9</i>										
$R_3 \times 10^{-3}$ ($\Omega \text{ cm}^2$)			696				462			9.06
$Q_3 \times 10^7$ (F/cm ²)			8.17				47.6			40.1
$Z_d \times 10^5$ (F)		23.8			1.93	0.22		7.95		2.03
<i>Sample PPh1</i>										
$R_3 \times 10^{-4}$ ($\Omega \text{ cm}^2$)									4.51	3.92
$Q_3 \times 10^5$ (F/cm ²)									3.70	5.04
<i>Sample PPh3</i>										
$R_3 \times 10^{-4}$ ($\Omega \text{ cm}^2$)						1.43				1.21
$Q_3 \times 10^6$ (F/cm ²)						2.43				1.58
$Z_d \times 10^3$ (F)							3.65	3.10		
<i>Sample PPh6</i>										
$R_3 \times 10^{-3}$ ($\Omega \text{ cm}^2$)									3.70	
$Q_3 \times 10^5$ (F/cm ²)									2.90	
$Z_d \times 10^3$ (F)					9.93					
<i>Sample PPh8</i>										
$R_3 \times 10^{-4}$ ($\Omega \text{ cm}^2$)						3.22			9.15	
$Q_3 \times 10^6$ (F/cm ²)						2.72			1.07	
<i>Sample PPh10</i>										
$R_3 \times 10^{-4}$ ($\Omega \text{ cm}^2$)						13.30				3.86
$Q_3 \times 10^5$ (F/cm ²)						5.61				2.69
$Z_d \times 10^4$ (F)				2.92						

Table 3

Evolution of the electrochemical parameters assumed to be associated with the cathodic processes

<i>t</i> (Days)	2	9	15	26	35	43	49	55	63	70
<i>Sample SWP1</i>										
$Z_d \times 10^4$ (F)						0.31	0.41	930		
<i>Sample SWP3</i>										
$R_3 \times 10^{-5}$ ($\Omega \text{ cm}^2$)			3.49		20.90		0.70			
$Q_3 \times 10^6$ (F/cm ²)			0.84		1.51		3.62			
$Z_d \times 10^3$ (F)						0.03		575		
<i>Sample SWP5</i>										
$Z_d \times 10^4$ (F)		0.11	0.10		0.16	0.26	3190			
<i>Sample SWP7</i>										
$R_3 \times 10^{-6}$ ($\Omega \text{ cm}^2$)				1.00						
$Q_3 \times 10^8$ (F/cm ²)				9.37						
$Z_d \times 10^4$ (F)		0.11	0.17		0.16			7800		
<i>Sample SWP9</i>										
$R_3 \times 10^{-5}$ ($\Omega \text{ cm}^2$)		3.78			5.90					
$Q_3 \times 10^7$ (F/cm ²)		4.08			12.30					
$Z_d \times 10^5$ (F)			4.64							

which the delaminated corroding area, A_d , (Figs. 1g, 2g, 3g and 4g) may be estimated by means of the following empirical equation:

$$A_d = \frac{C_{dl}(t)}{20} \quad (2)$$

where A_d is the delaminated area (cm²), $C_{dl}(t)$ is the electrochemical double layer capacitance measured at any time t (μF) and 20 is the typical value of the bare steel double layer capacitance, adopted to estimate the underlying metallic active surface ($\mu\text{F}/\text{cm}^2$). The A_d cyclic behavior is typical for defective coatings with a permanent change of plugged and free pores [12–16].

With regard to the electrochemical parameters R_{ct} and C_{dl} , and the delaminated area evolution, Figs. 1–4 illustrate that once the barrier protection of the coating is lost, the E_{corr} reaches (or remains at) a ‘plateaux’ near to -0.6 ± 0.05 V/SCE and R_f stabilizes between 10^3 and $10^4 \Omega \text{ cm}^2$. But, the changes in the electrochemical interface behavior may be significant leading, in most cases, to highly delaminated (i.e. electrochemically active) areas and, therefore, underlying steel corrosion. Throughout the exposure test, the kinetics and magnitude of both the resistive and capacitive changes associated with the corrosion process taking place at the steel/chlorinated rubber paint interface show a certain dependence on the substrate surface treatment. Thus, the R_{ct} and C_{dl} values either fluctuate between 3 and 4 orders of magnitude or else stay almost steady, showing well differentiated dynamics of the delamination growth. These results, together with the sometimes appearing Q_3 and R_3 components linked in series with the diffusional Z_d component – see Tables 2 and 3 – suggest the presence of a mixed diffusion and charge transfer controlled process. It is assumed that such components would be intimately related with the bad corrosion performance of the coated steel but, particularly, with the kinetics of the reaction(s) occurring at the cathodic areas, mainly the oxygen diffusion through

the film, its reduction reaction and/or the OH^- diffusion through the interfacial aqueous layer. In order to obtain further insight into the correct physical and electrochemical interpretation of such a circuit, more investigations are currently in progress so no further explanations will be given here.

The experimental results from the differently surface treated steel sheets/80 μm chlorinated rubber paint/artificial seawater systems show that the P and PPh samples remain unchanged and display a high corrosion protection level throughout the test, with values of E_{con} near to 0 ± 0.1 V/SCE, $R_f \geq 10^7 \Omega \text{ cm}^2$, $C_f < 10^{-9} \text{F}/\text{cm}^2$, water absorption $\leq 1\%$ and C_{dl} , and R_{ct} tending toward zero and infinity, respectively. However, as can be seen in Figs. 1–4 the S samples and to a lesser extent the SWP samples, do not give a good protective performance. Therefore, under the current experimental conditions a ranking of the corrosion protection as a function of the different pretreatments leads to the following results: PPh \geq P \geq SWP $>$ S for thick chlorinated rubber films and PPh $>$ P $>$ S \equiv SWP for thin films.

4. Discussion

Tests accomplished under free corrosion conditions show the influence of both the paint coating barrier effect and the surface preparation procedure on the protective ability. A large amount of diverse data has been gathered using an electrochemical technique, then fitted by means of mathematical algorithms arising from electrical equivalent circuit models, and interpreted on the basis of their correlation with physicochemical processes occurred in pretreated steel/chlorinated rubber paint/artificial seawater systems.

Thus, examination of the experimental results, coming from such freely corroding systems and summarized in Figs. 1–4 and Table 3, show that the extent of protection at any stage is much higher and stable when the thick poly-

mer film is applied on P and PPh than on S and SWP samples. This is attributed to a good barrier protection provided by the paint film. It reduces the permeation of corrosion enough to induce chemicals such as water, oxygen and ions through the film to impede, if not eliminate, a continuous cathodic reaction. This is improved by the following mechanisms: (a) on surfaces cleaned by acid derusting (i.e. P samples), all the rust particles are removed causing not only an enhancement on the metal/coating adhesion but also the absence of a salt water soluble layer on the steel surface which will undoubtedly retard the formation of an electrolytic layer at the metal/coating interface (due to a reduced, if any, osmotic effect) during immersion, and (b) on PPh samples, the phosphate coating forms complex metallic compounds with the steel substrate having good ability to resist corrosion [17]. This last surface pretreatment provides high surface roughness allowing stronger mechanical adhesion forces at the phosphated/paint interface and, therefore, also enhancing the resistance to coating delamination.

In agreement with these mechanisms, it is assumed that the steel surface stays effectively isolated from the electrolyte solution throughout the exposure time. Referring to the same type of steel sheets coated with thinner more defective paint films, the Figs. 1–4 also report: (a) a less significant difference among sample behavior, (b) the evolution of all the electrical and electrochemical parameters with the immersion time account for a more or less severe coating deterioration and corrosive attack whose kinetics are dependent on the type of surface preparation used and (c) the lost of corrosion protective properties through a series of physicochemical processes make all these samples unsuitable for exposure conditions similar to the actual experimental ones. It is important to denote that PPh samples exhibited a delay time for the first 20–25 days of immersion. Neither corrosion nor disbonding can be detected. Nevertheless, as with the rest of the samples, once this process starts it advances at a rate which either increases with time or becomes zero, Fig. 3g. Such a delay time is attributed to the above mentioned temporary corrosion resistant properties of the porous phosphated layer. The disbonding growth is probably due to the cathodic reaction process, mainly the oxygen reduction reaction forming hydroxyl ions which has been suggested to destroy the interfacial bond [18].

It is interesting to compare the water absorption values and the corrosion protection properties of the different coated steel samples in artificial seawater. Thus, the higher absorption values together with the anomalous polymer capacitance trend, strongly increase as the immersion time elapses (Figs. 1f, 2f, 3f, 4f, 1d, 2d, 3d and 4d, respectively). This can be justified by assuming water penetration into the paint/treated steel interface. Besides, these results correlate quite well with the trend of both the delaminated area (Figs. 1g, 2g, 3g and 4g) and E_{corr} of the coated steel (Figs. 1a, 2a, 3a and 4a) as well as with R_f of the chlorinated rubber film as a function of the exposure time, (Figs. 1b, 2b, 3b and 4b). Such a correlation can also be observed with R_{ct} (associated

with the underlying steel corrosion rate) and C_{dl} contributions which vary inversely and directly, respectively, with the extent of the metallic active area, as can be seen in Figs. 1c, 2c, 3c, 4c, 1e, 2e 3e and 4e.

Furthermore, the substrate corrosion is accompanied by an activated transport of species through the organic coating film so that the electroneutrality condition can be performed. If the ionic current through the film is concentrated at this active area, it may be assumed that the R_f value is influenced by three different factors. First, the amount of water absorbed (Figs. 1g, 2g, 3g, 4g) diminishes the barrier energy in order that the mass transport process takes place easier. Second, the amount of electrical charge developed into the non-hydrophilic tested chlorinated rubber films which makes them behave like a semipermeable membrane [19] and third, by the extent of the delaminated area.

Some uncertainties cause difficulties in interpreting univocally the different combination of elements in the impedance networks describing impedance data changes in freely corroding pretreated coated steel interfaces. However, the agreement between the experimental evidence and the state of the samples determined through periodical visual inspections provide some proof of the susceptibility of the tested samples to corrode and delaminate when exposed to seawater.

5. Conclusions

The agreement between electrochemical and periodic visual inspection results demonstrate that the impedance measurements are sensitive enough to report changes introduced on the coated steel corrosion performance when different surface preparation techniques are used. Furthermore, it is also shown that the interpretation of experimental data fitted using equivalent circuit models turns increasingly complicated as the dynamic changes in the physicochemical processes occurring at the coated metal/electrolyte solution interface take place. Therefore, more efforts are being developed in order to obtain insights related not only with the kinetics parameters characterization but also with the intrinsic nature of such processes.

The corrosion behavior of chlorinated rubber painted steel exposed to artificial seawater correlates well with the water absorption percentage, the delaminated area and the membrane ionic resistance performance. Among the surface preparation techniques tested, the best corrosion protection level is provided by pickled + phosphated painted steel surfaces followed by the pickled surfaces. By comparing these results with those corresponding to the sandblasted and sandblasted + wash primer samples, it was concluded that not only a stable, corrosion resistant and adhesion enhancing layer formed on the steel substrate but also a free from rust treated steel surface must be obtained in order for its useful life to be lengthened. Besides, a permselective organic coating film must be also applied, thick enough to

provide significant barrier protection, at least, under exposure conditions including aqueous solutions containing high chloride concentrations.

Acknowledgements

D.M.S., CIC Fellow; P.R.S., CIC Fellow, UNLP; C.I.E., CONICET Researcher, UNLP; A.R.D.S., CIC Researcher. The authors gratefully acknowledge the Comisión de Investigaciones Científicas de la Provincia de Buenos Aires (CIC) and the Consejo Nacional de Investigaciones Científicas y Técnicas (CONICET) for their financial support for this research work.

References

- [1] V.M. Ambrosi and A.R. Di Sarli, *Anti Corros.*, October (1993) 9.
- [2] B.A. Boukamp, Report CT88/265/128, CT89/214/128, University of Twente, Netherlands, 1989.
- [3] G.W. Walter, *Corros. Sci.*, 32 (1991) 1059.
- [4] H. Leidheiser, Jr., *J. Coat. Technol.*, 63 (1991) 21.
- [5] P.R. Seré, D.M. Santágata, C.I. Elsner and A.R. Di Sarli, *Surf. Coat. Int.*, (1998) in press.
- [6] L. Hartshorn, N.J.L. Megson and E. Rushton, *J. Soc. Chem. Ind.*, 56 (1937) 266T.
- [7] D.M. Brasher and A.H. Kingsbury, *J. Appl. Chem.*, 4 (2) (1954) 62.
- [8] H. Leidheiser, Jr. and M.W. Kendig, *Corrosion*, 32 (1976) 69.
- [9] R.A. Armas, S.G. Real, C. Gervasi, A.R. Di Sarli and J.R. Vilche, *Corrosion*, 48 (1992) 379.
- [10] T. Szauer and A. Brandt, *J. Oil Col. Chem. Assoc.*, 67 (1984) 13.
- [11] D.J. Frydrych, G.C. Farrington and H.E. Townsend, in M.W. Kendig and H. Leidheiser, Jr. (eds.), *Corrosion Protection by Organic Coatings*, Vol. 87-2, The Electrochemical Society, Pennington, NJ, 1987, p. 240.
- [12] G.W. Walter, *J. Electroanal. Chem.*, 118 (1981) 259.
- [13] N. Pébere, T. Picoud, M. Duprat and F. Dabosi, *Corros. Sci.*, 29 (1989) 1073.
- [14] J. Titz, G.H. Wagner, H. Spähn, M. Ebert, K. Jüttner and W.J. Lorenz, *Corrosion*, 46 (1990) 221.
- [15] G. Reinhard and U. Rammelt, *Plaste Kautsch.*, 31 (1984) 312.
- [16] J.C. Rowlands and D.J. Chute, *Corros. Sci.*, 23 (1983) 331.
- [17] *ASM Handbook, Corrosion*, Vol. 13, ASM International, 1992.
- [18] H. Leidheiser, Jr., *Prog. Org. Coat.*, 7 (1979) 79.
- [19] D.Y. Perera and P.M. Heertjes, *J. Oil Col. Chem. Assoc.*, 54 (1971) 313; 54 (1971) 395; 54 (1971) 546; 54 (1971) 774.